Production of SiO and Si(^{3}P) Atom in the Reaction of Silane with O(^{1}D)

Atsuko Takahara,† Atsumu Tezaki,* and Hiroyuki Matsui

Department of Mechanical Engineering, The University of Tokyo, 7-3-1 Hongo, Bunkyo-ku, Tokyo 113-8656, Japan

Received: March 24, 1999; In Final Form: October 11, 1999

The mechanism of SiO production in the reaction of O(^{1}D) with SiH_4 is reinvestigated, where O(^{1}D) is produced by the 193 nm photolysis of N_2O and nascent distribution of SiO ($v = 0-8$) is determined by using a laser-induced fluorescence (LIF) detection system. Improvement of the reliability of the data is attained by using a simple tunable optical parametric oscillator system, since this system can cover the progression of the LIF spectrum over a wide range of wavelengths within a single scan. Nascent vibrational distribution of SiO is approximately expressed by a Boltzmann distribution of about $T_v = 5200$ K. Also, the Si(^{3}P) atom is identified as a direct product of this reaction, although the branching fraction is estimated to be only 3×10^{-4} of the total products. The mechanism of the formation of SiO is discussed by comparing the observed nascent vibrational distribution with that calculated by a quasi-static theory for the multiple-step unimolecular decomposition of chemically activated silanol.

Introduction

The chemical kinetics of silane and its derivatives have long been studied extensively because of their importance in the microelectronic fabrication processes and the safety problems related to their hazardous nature.[1−15] However, the accumulated information on the rates and mechanisms for the reactions of silicon-containing species still seems insufficient. In particular, direct experimental studies of the reactions of species composed of Si−H−O atomic systems have been scarce, since most of the stable molecules of such a system are not easily available at ambient conditions. The deficiency may be partly compensated by using a chemical activation method; for example, the unimolecular decomposition reaction of highly excited silanol (SiH_3OH) was examined in our previous study by using the insertion reaction of O(^{1}D) into a Si−H bond of SiH_4.[14] The reaction of O(^{1}D) with SiH_4

$$O(^1D) + SiH_4 \rightarrow \text{products} \qquad (1)$$

was shown in our previous study to have many product channels, and the branching fractions of H, OH, and SiO were determined as 0.36, 0.24, and 0.07−0.13, respectively. Recently, a crossed molecular beam study was conducted on the O(^{1}D) + SiH_4 reaction and it is demonstrated that H_3SiO is observed with backward angular distribution in the H + H_3SiO reaction channel and that the production of OH has an angular distribution of the forward scattering for the reaction channel of OH + SiH_3.[15] Also, the nascent vibrational energy distribution measured in our previous work by using a laser-induced fluorescence (LIF) method is found to be highly inverted, i.e., [OH($v'' = 1$)]/[OH($v'' = 0$)] = 1.52.[14] Therefore, OH and H may be produced by direct mechanisms such as abstraction and substitution reactions rather than the unimolecular decomposition of silanol.

The production of SiO has been also confirmed in the crossed molecular beam experiment. In contrast to H and OH, the angular distribution of the products $2H_2$ + SiO is close to isotropic; thus, the lifetime is suggested to be longer than the rotational period. The experimental result supports that SiO is produced by the unimolecular decomposition of SiH_3OH, where the chemical energy may be randomly partitioned in SiH_3OH, as well as in other reaction intermediates involved with SiO formation. Chemically activated silanol produced in the reaction 1 may decompose consecutively to a variety of products such as

$$O(^1D) + SiH_4 \rightarrow (SiH_3OH)^*$$

$$\rightarrow SiH_3 + OH \qquad \Delta H_{298K} = -236 \text{ kJ/mol} \qquad (1a)$$

$$\rightarrow H_3SiO + H \qquad \Delta H_{298K} = -238 \text{ kJ/mol} \qquad (1b)$$

$$\rightarrow H_2SiOH + H \qquad \Delta H_{298K} = -365 \text{ kJ/mol} \qquad (1c)$$

$$\rightarrow SiH_2 + H_2O \qquad \Delta H_{298K} = -437 \text{ kJ/mol} \qquad (1d)$$

$$\rightarrow H_2SiO + H_2 \qquad \Delta H_{298K} = -571 \text{ kJ/mol} \qquad (1e)$$

$$\rightarrow HSiOH + H_2 \qquad \Delta H_{298K} = -565 \text{ kJ/mol} \qquad (1f)$$

$$\rightarrow SiO + 2H_2 \qquad \Delta H_{298K} = -575 \text{ kJ/mol} \qquad (1g)$$

$$\rightarrow Si + H_2 + H_2O \qquad \Delta H_{298K} = -264 \text{ kJ/mol} \qquad (1h)$$

$$\xrightarrow{+M} SiH_3OH \qquad \Delta H_{298K} = -755 \text{ kJ/mol} \qquad (1i)$$

where the heats of formation are mainly taken from the ab initio calculations conducted by Zachariah et al.[8] Other theoretical studies also support the possibilities of the reactions 1a−1f.[8−13]

In this paper, the nascent vibrational distribution of SiO produced in the reaction of SiH_4 + O(^{1}D) is reinvestigated by using an improved system of the LIF measurement in order to examine the dynamics of this unique reaction because previous results on the vibrational energy distribution of SiO by using a dye laser system had a large scatter due to the difficulty of

† Present address: Institut für Physicalische Chemie, Universität Göttingen, Tammannstr. 6, D-37077 Göttingen, Germany.

10.1021/jp9910237 CCC: $18.00
Published on Web 12/03/1999

conducting successive scans over a wide range of wavelengths. An accurate measurement for the nascent distribution is essential for the examination of the reaction mechanism. A comparison with the prior distribution based on the conventional statistical theory is also performed for the multiple-step unimolecular decomposition of energized silanol as a standard procedure. In addition, another unexpected product, Si(^{3}P) atom by reaction channel 1h is also confirmed in this study. The product branching fractions and the reaction pathways for Si production are discussed.

Experimental Section

An experiment using a laser-photolysis pump and an LIF probe technique was conducted in a quasi-static flow cell. An optical parametric oscillator (OPO; Continuum, Surelite OPO) was used as the probe light source. This OPO laser was pumped by a frequency-tripled Nd:YAG laser (Continuum, Surelite-II YAG) to generate tunable outputs of "signal" at 420−700 nm and "idler" at 720−2300 nm at the same time. The visible OPO "signal" was further frequency-doubled with a BBO crystal to observe vibrational distributions of SiO in the 230−285 nm region. For scanning the wavelength, the doubling crystal and the OPO crystal were synchronously rotated by a pair of homemade PC-controlled mechanical devices. The OPO system used in this study had no dispersing optics such as a grating; therefore, the line width of the visible output was rather wide (typically 50 cm^{-1} according to the manufacturer's specification). However, the line width of the UV probe was reduced (4 cm^{-1} at 230 nm to 7 cm^{-1} at 300 nm) because of nonlinearity and the phase-matching condition for the doubling crystal. This width is still quite wide compared to that of typical dye lasers or narrowband OPOs. Nevertheless, it has sufficient resolution to discriminate most of the vibrational bands of SiO. This setup has a merit that one can quickly scan the output over a wide range of wavelengths without replacing the optical parts, or without adjusting the optical alignment, so that spectra of reproducible intensities are easily obtained within a relatively short time.

Mixtures of N_2O and SiH_4 diluted in He were flowed in a cell (23 mm i.d.) and were irradiated by 193 nm ArF excimer laser (Lambda Physik, Compex 102) pulses coaxially with the flow, where N_2O is photolyzed to produce O(^{1}D). A typical fluence of the photolysis pulse was 10 mJ/cm^2 at the observation point. Fluorescence from SiO was transmitted through a selected UV band-pass filter, detected by a photomultiplier tube, and then acquired by a boxcar integrator. Assuming a plug−flow condition, the gas residence time between the inlet and the observation point was estimated to be 80 ms at a typical overall flow rate of 200 sccm and 10 Torr total pressure, while the lasers were operated at 10 Hz repetition. All the experiments were carried out at room temperature (295 ± 3 K).

Results and Discussion

A. Nascent Vibrational Distribution of SiO. An example of the LIF spectrum demonstrating production of vibrationally excited SiO in the reaction of SiH_4 + O(^{1}D) is shown in Figure 1, where A−X bands of $v'' = 0-8$ are assigned unambiguously. In this example, the probe delay was fixed at 20 μs after the photolysis; 75% of O(^{1}D) is consumed at this time by reactions with SiH_4 and N_2O under the employed reactant concentrations.

Time-dependent traces of SiO at the vibrational levels (0−5) are demonstrated in Figure 2. As shown in this figure, the rapid rise of the signal intensity corresponds to the production process of SiO. The initial rise rate is plotted against the

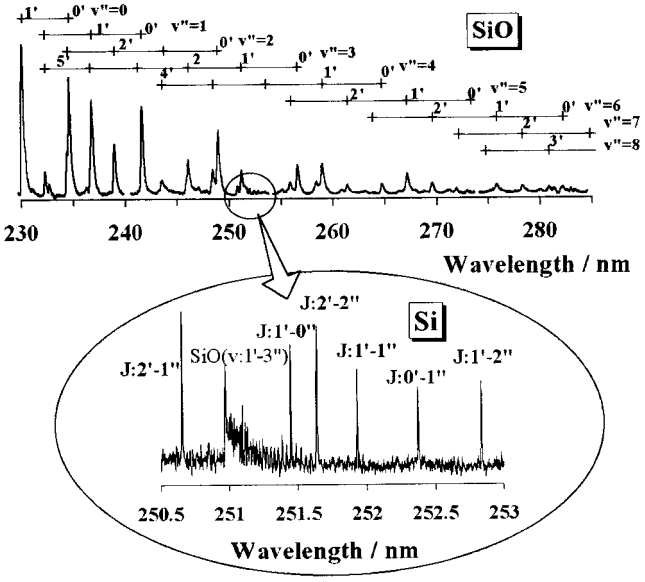

Figure 1. LIF spectra observed in the ArF laser photolysis of 5 mTorr of SiH_4 and 10 mTorr of N_2O mixture diluted in 10 Torr of He. A frequency-doubled OPO laser is used for the upper trace, showing ($A^1\Pi-X^1\Sigma^+$) ($v'-v''$) bands of vibrationally hot SiO. A frequency-doubled dye laser of relatively high resolution is used for the lower trace in the frame, showing Si(^3P_J) lines superimposed over the (1′−3″) band of SiO.

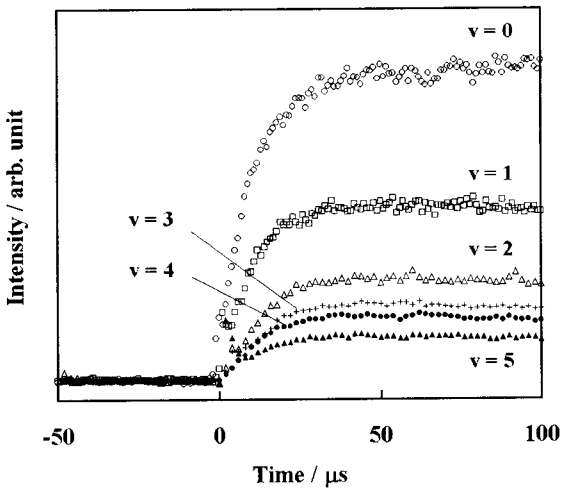

Figure 2. Time profiles of SiO in the vibrational states 0−5 from the photolysis of 5 mTorr of SiH_4/10 mTorr of N_2O mixture in 10 Torr of He. Signal intensities are scaled as observed and only roughly represent the vibrational populations.

concentration of SiH_4 and then gives the overall rate constant for reaction 1 by using a pseudo-first-order analysis. It is found that the rate constants determined in this way lie in the range (2.6−3.0) × 10^{-10} cm^3 $molecule^{-1}$ s^{-1} for all the observed vibrational levels. Consequently, it is essentially independent of the vibrational level and agrees very well with the consumption rate of O(^{1}D) measured by using a vacuum ultraviolet (VUV) LIF method in our previous study. It is thus reconfirmed that SiO is a kinetically direct product of reaction 1. From the time dependence measurements, vibrational relaxation of SiO is found to be much slower. Nevertheless, the coupling of the production of SiO and successive relaxation is taken into account in the present analyses for determination of the vibrational distribution at $t = 0$. The results for the state-specific vibrational relaxation rate of SiO will be reported in a separate publication.[16]

Integrated intensities of the observed SiO vibrational bands are converted into the relative vibrational population by using

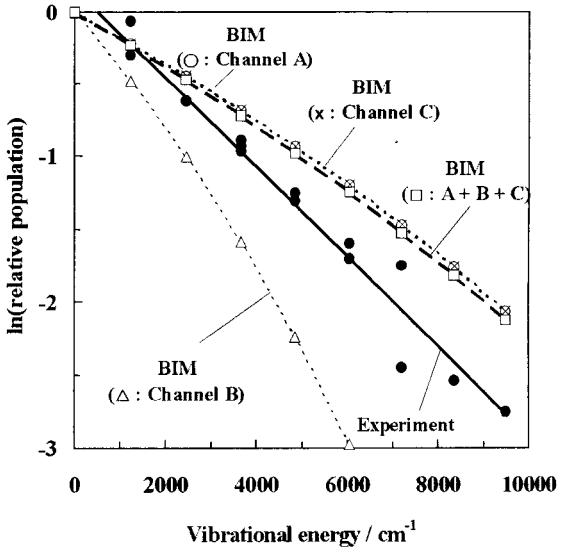

Figure 3. Observed and calculated nascent vibrational distributions of SiO produced in the $SiH_4 + O(^1D)$ reaction. Solid circles are experimental data, and a solid line is a linear regression fit representing a vibrational temperature of 5200 K. Open symbols and dashed lines are results of model calculations described in the text.

reported SiO (A−X) Franck−Condon factors,[17] with corrections for the wavelength dependence of the photomultiplier sensitivity and the transmittance of the filters. Since some bands are overlapped by weaker ones of different transitions, small contributions from the minor peaks are corrected using an iteration procedure until the observed intensity ratios are reproduced by the nascent vibrational distribution given as a guess. As shown in Figure 3, the evaluated nascent vibrational distribution analyzed in this way is approximately given by the Boltzmann distribution with a vibrational temperature $T_v = 5200 \pm 660$ K (2 × standard deviation). This result is substantially higher than the estimates of the previous study at 3900 K[14] obtained by using a dye laser source for the LIF system. It is clear that the experimental error in estimating the vibrational population has been reduced in the present study.

B. Detection of Triplet and Singlet Silicon Atom. The ground-state Si(^3P_J) was observed by $4s(^3P_{J'})-3p^2(^3P_{J''})$ transitions lying at 250−253 nm for ArF laser irradiation into N_2O/SiH_4 mixture as shown in the inset in Figure 1. Here, the Si atom was detected by using a dye laser probe system having relatively higher resolution than the OPO system.

To confirm that the observed Si(^{3}P) atom is a direct product of the $SiH_4 + O(^1D)$ reaction, the time dependence of the Si(^{3}P) atom was monitored and kinetic analyses for the dependence on the concentrations of SiH_4 and N_2O were performed. The difference of the time dependence between spin−orbit angular quanta $J = 0-2$ was not observed because of the rapid energy-transfer process among these energy levels. The most intense ($2'-1''$) line at 250.7 nm was mainly used for the kinetic examination. It is also noted that this line has no interference from SiO($v'-v''$) bands.

The profile of the Si(^{3}P) atom has rise and decay components and is dependent on both SiH_4 and N_2O concentrations as shown in parts a and b of Figure 4, respectively. The profile is fitted to the following double-exponential function:

$$X = X_0[\exp(-k_d t) - \exp(-k_r t)]$$

where the rise rate k_r is inevitably larger than the decay rate k_d. The rates thus obtained are plotted against the concentrations of SiH_4 and N_2O in parts a and b of Figure 5, respectively.

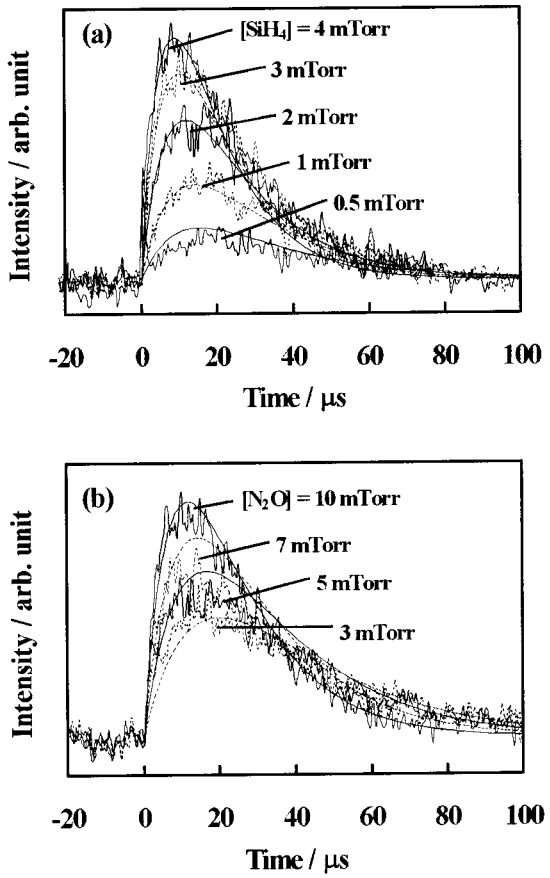

Figure 4. Time profiles of Si atom LIF at $J = 2'-1''$ transition in the photolysis of SiH_4/N_2O mixtures: (a) at fixed [SiH_4] (3 mTorr) and indicated [N_2O]; (b) at fixed [N_2O] (10 mTorr) and indicated [SiH_4]. Smooth lines are calculated with eq 5.

If Si(^{3}P) is a direct product of $SiH_4 + O(^1D)$, generation and consumption of Si initiated by the photolysis of N_2O can be described as

$$N_2O + h\nu \rightarrow O(^1D) + N_2 \quad (0)$$

$$O(^1D) + SiH_4 \rightarrow \phi Si + \text{other products} \quad (1)$$

$$O(^1D) + N_2O \rightarrow \text{products} \quad (2)$$

$$Si + SiH_4 \rightarrow \text{products} \quad (3)$$

$$Si + N_2O \rightarrow \text{products} \quad (4)$$

Since $O(^1D)$ is a minor species relative to SiH_4 and N_2O, a pseudo-first-order analysis gives the time dependence of the concentration of Si atom as follows:

$$[Si] = \phi k_1[SiH_4]\sigma[N_2O]\frac{\exp(-k_O t) - \exp(-k_S t)}{k_S - k_O} \quad (5)$$

where k_O is the rate of $O(^1D)$ consumption, $k_O = k_1[SiH_4] + k_2[N_2O]$, k_S is the rate of Si consumption, $k_S = k_3[SiH_4] + k_4[N_2O]$, and σ is the photolysis yield of $O(^1D)$ from N_2O. Because of the symmetric nature of eq 5 in terms of k_O and k_S, the corresponding order with k_r and k_d can be altered according to the sign of $(k_S - k_O)$. The present observations are accounted for when $(k_S - k_O)$ is assumed to be positive; that is, k_S and k_O correlate to the rise and the decay parts, respectively. The slope of k_d against [SiH_4], i.e., 3.0×10^{-10} cm^3 molecule^{-1} s^{-1}, is

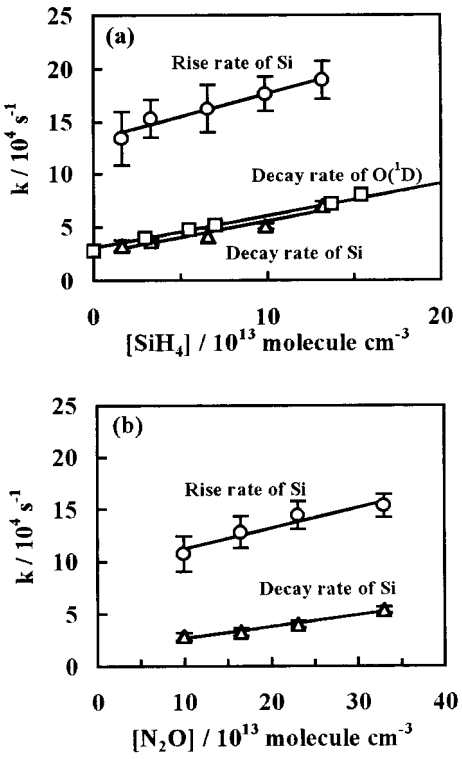

Figure 5. Pseudo-first-order rise and decay rates in the double-exponential fit of the Si time profiles: (a) as a function of N_2O concentrations and (b) as a function of SiH_4 concentrations. Also shown with open squares in (a) are the decay rates of $O(^1D)$ observed in the former study.[14]

TABLE 1: Reaction Rate Constants Relevant to Production and Consumption of Si Atom in the Photolysis of SiH_4/N_2O Mixture

reaction	rate constant (10^{-10} cm^3 molecule^{-1} s^{-1})	temperature (K)	reference
1 $O(^1D) + SiH_4$	3.0 ± 1.0	295 ± 3	this work
	3.0 ± 0.3	295 ± 3	Okuda[7]
2 $O(^1D) + N_2O$	1.1 ± 0.2	295 ± 3	this work
	1.16 ± 0.35	200−300	DeMore[19]
	1.16	200−350	Atkinson[20]
3 $Si + SiH_4$	4.4 ± 1.0	295 ± 3	this work
	3.5 ± 1.0	320	Tanaka[18]
4 $Si + N_2O$	2.0 ± 0.75	295 ± 3	this work
	0.82 ± 0.41	350	Swearengen[21]
	1.9 ± 0.2	300	Husain[22]

thus considered to be the rate constant k_1, since it is exactly the same as the consumption rate of $O(^1D)$ by the reaction with SiH_4, as shown in Figure 5a and in Table 1. Similarly, the dependence of k_r against $[SiH_4]$ gives $k_3 = 4.3 \times 10^{-10}$ cm^3 molecule^{-1} s^{-1}, which is in good agreement with the value that was measured in a plasma reactor.[18]

In addition, from the slopes of k_d and k_r against $[N_2O]$, k_2 and k_4 are determined as 1.2×10^{-10} and 2.0×10^{-10} cm^3 molecule^{-1} s^{-1}, respectively. They are in reasonable agreement with literature values for k_2[19,20] and k_4.[21,22] Also, as shown by the solid curves in parts a and b of Figure 4, the observed dependence of the relative signal intensity on the initial concentrations of SiH_4 and N_2O is completely reproduced with eq 5. It seems reasonable, therefore, to consider that $Si(^3P)$ is a direct product of reaction 1. The rate constants of reactions 1−4 determined in this study are summarized in Table 1, together with those of previous studies for comparison.

By use of the oscillator strengths of Si [23] and SiO [24] and the Franck−Condon factor for SiO,[17] the fractional yield for $Si(^3P)$ is also estimated by comparing the integrated fluorescence intensity of Si with that of the $SiO(1'-3'')$ band monitored in the same run as shown in Figure 1. The relative production yield of $Si(^3P)$ against SiO is evaluated to be 2.3×10^{-3}, where consumption of Si by the reactions with SiH_4 and N_2O, as well as the measured vibrational distribution of $SiO(v)$, is taken into account in the analysis of the integrated intensity of the spectra.

It should be noted that the magnitude of the oscillator strength of the A−X transition of SiO has not been completely fixed yet. Here, $f_{SiO} = 0.103$ from a theoretical evaluation of Oddershede and Smith[24] is employed to evaluate the branching fraction for SiO, since this is consistent with the fluorescence lifetime of SiO(A) measured directly by Suzuki.[25] This choice gives the product branching fraction of SiO as 0.13, which is in good agreement with the estimation in the crossed beam experiment.[15] Consequently, the branching fraction of Si production in the reaction of $O(^1D) + SiH_4$ is given as 3×10^{-4}.

$Si(^1D)$ can be also a direct product of the reaction 1, since it does not violate the total spin conservation during the reaction. In this case, the observed $Si(^3P)$ atom can be produced as a result of the quenching of the initial product $Si(^1D)$. As a consequence, $Si(^1D)$ was detected by the $4s(^1P^O_1)-3p^2(^1D_2)$ transition at 288.16 nm in the N_2O/SiH_4 mixture after the irradiation by the 193 nm pulse. However, this was not ascribed to a product of the title reaction because the rise of $Si(^1D)$ was found to be within 1 μs, i.e., much faster than predicted from the collisional process and the experimental time profile, and is much inconsistent with the calculated one for the reactions 1−4. $Si(^1D)$ was supposed to be generated by the photolysis of some residual species including Si in the cell. The amount of $Si(^1D)$ is also estimated to be an order of magnitude less than that of the $Si(^3P)$ atom by using the same procedure as above. Therefore, the quenching of observed $Si(^1D)$ is concluded to give no influence on the time dependence of $Si(^3P)$.

The branching fractions of the products of reaction 1 are summarized in Table 2, together with our previous experimental results.

C. Analysis of Multiple-Step Decomposition Process of Activated Silanol. From the above discussion, it may be reasonable to assume that SiO and $Si(^3P)$ are produced through the decomposition of silanol formed by the insertion of $O(^1D)$ into a Si−H bond of SiH_4. The insertion mechanism of $O(^1D)$ has been supported by former studies[26,27] for its reactions with hydrocarbons and other compounds. Owing to the large excess energy, various product channels are energetically allowed, as is already mentioned. However, the reaction mechanism of SiO formation is probably not straightforward, but multiple-step decomposition channels such as

$$(H_3SiOH)^* \rightarrow TS1 \rightarrow HSiOH + H_2 \rightarrow TS2 \rightarrow SiO + 2H_2 \quad \text{(A)}$$

$$(H_3SiOH)^* \rightarrow TS3 \rightarrow H_2SiO + H_2 \rightarrow TS4 \rightarrow SiO + 2H_2 \quad \text{(B)}$$

$$(H_3SiOH)^* \rightarrow TS3 \rightarrow H_2SiO + H_2 \rightarrow TS5 \rightarrow HSiOH + H_2 \rightarrow TS2 \rightarrow SiO + 2H_2 \quad \text{(C)}$$

may be responsible. These reaction pathways are schematically shown in the energy diagram in Figure 6. If the excited intermediates, i.e., H_3SiOH, H_2SiO, and HSiOH have sufficiently long lifetimes to randomize the excess energy, the prior energy distributions of fragments are calculated by using the

TABLE 2: Product Branching Fractions in Reaction O(^{1}D) + SiH_4

product	fraction	methodology	reference
SiO	0.07−0.13[a]	spectral intensity, SiO(2′−0″) vs NO(0′−0″)	Okuda[7]
Si(^{3}P)	3×10^{-4}	spectral intensity, Si(^{3}P) vs SiO(1′−3″)	this work
OH	0.36	relative yield against reference reaction O(^{1}D) + H_2	Okuda[7]
H	0.24		Okuda[7]

[a] 0.13 is recommended in this paper.

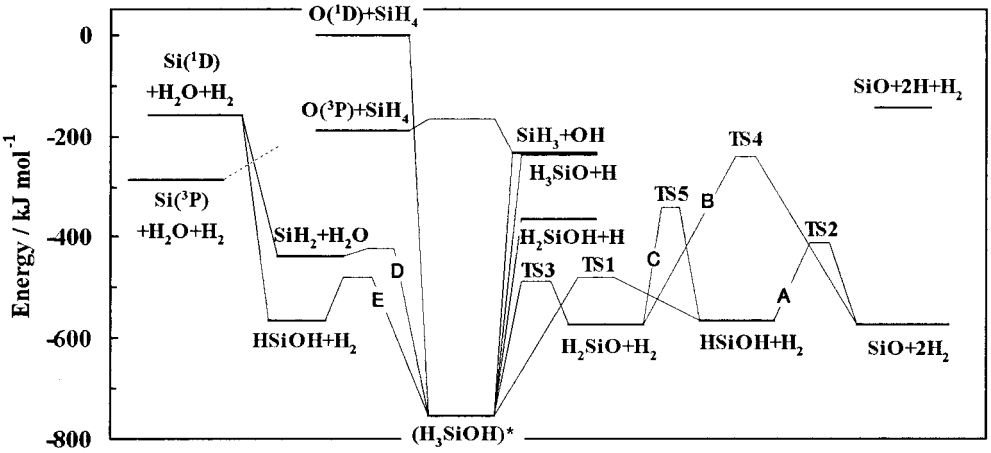

Figure 6. Energy level diagram showing product branching pathways of the SiH_4 + O(^{1}D) reaction. Energies of species and transition states are mainly referenced to the ab initio study of Zachariah and Tsang.[8]

TABLE 3: Reaction Rates and Branching Fractions for Channels Forming SiO + $2H_2$ by the BIM/RRKM Model for Multiple-Step Unimolecular Decomposition of Activated Silanol

	channel A	channel B	channel C
first step decomposition	$H_3SiOH \rightarrow TS1 \rightarrow HSiOH + H_2$	$H_3SiOH \rightarrow TS3 \rightarrow H_2SiO + H_2$	
k_r[a] (s^{-1})	1.0×10^{12}	3.7×10^{11}	
second step	$HSiOH \rightarrow TS2 \rightarrow SiO + H_2$	$H_2SiO \rightarrow TS4 \rightarrow SiO + H_2$	$H_2SiO \rightarrow TS5 \rightarrow HSiOH$
k_r[a] (s^{-1})	5.4×10^9	2.2×10^9	5.1×10^9
third step			$HSiOH \rightarrow TS2 \rightarrow SiO + H_2$
T_v(SiO)[b] (K)	5700	2700	5600
fraction in overall SiO	0.72	0.06	0.22

[a] k_r is the microcanonical RRKM reaction rate. [b] Calculated by BIM.

conventional statistical theory. In this study, the internal energies of the reaction intermediates and products are calculated by using the barrier impulsive model (BIM).[28] In this model, it is assumed that the reactant internal energy is statistically partitioned at the transition state (TS) for all the degrees of freedom; however, the potential energy released after passing the TS is simply given to the intermolecular translational motion and products rotations. When enough vibrational energy is partitioned into the second intermediate, HSiOH in the reaction channel A for example, the successive decomposition forming SiO + H_2 is energetically allowed. The energy distribution in SiO and H_2 is evaluated by using the first-step product energy distribution. The statistical calculations can be conducted in a standard way using given vibrational frequencies and moments of inertia for the intermediates, products, and transition states.[8]

RRKM calculations are also conducted to estimate the rates and the branching ratios for these possible reaction channels by using the same information for the molecular structures and the energies of the transition states.

The calculated results of the product energy distributions and branching fractions for the assumed channels are summarized in Table 3. Calculated vibrational distributions of SiO assuming channels A, B, and C are compared with the measured nascent distribution in Figure 2. It is found that both channels A and C give slightly larger vibrational energies, but they are in reasonable agreement with that of present experimental result, since the difference is almost within the limit of uncertainty of the experiment. On the other hand, channel B gives much lower vibrational energy because of the higher exit barrier. It seems impossible to discriminate channels A and C from only the observed vibrational distribution; however, channel A (HSiOH intermediate) is more favorable for the production of SiO by the consideration of relative rates based on the RRKM calculations.

For the production of the Si(^{3}P) atom, H_2 and H_2O are supposed to be the counterparts of the product. Hence, two distinctly different channels, i.e., H_2O is produced prior to H_2 or vice versa, can be expressed as follows:

$$(H_3SiOH)^* \rightarrow SiH_2 + H_2O \rightarrow Si + H_2 + H_2O \quad \text{(D)}$$

$$(H_3SiOH)^* \rightarrow HSiOH \text{ (or } H_2SiO) + H_2 \rightarrow Si + H_2O + H_2 \quad \text{(E)}$$

As is indicated, Si(^{3}P) is a product of the reaction 1; then crossing from singlet to triplet surface should be included in these reaction pathways. Shock tube studies have already shown that Si(^{3}P) + H_2 is a product channel in the thermal decomposition of SiH_2 via intersystem crossing without having too high a barrier compared to the endothermicity of the reaction.[29−31] The spin conservation rule is generally moderated for systems including a heavy atom like Si.

By application of the same BIM procedure, the product branching fractions for Si(^{3}P) is estimated for both channels D

and E as 1.6×10^{-2} and 5×10^{-4}, respectively, where the second-step decomposition of HSiOH and SiH_2 is treated as barrierless and the effect of the intersystem crossing is disregarded.

Although it is impossible to judge which channel is dominant for production of the Si atom, it implies that the production of Si at this small yield is by no means a mystery for the unimolecular decomposition of highly excited SiH_3OH.

Conclusions

Through our previous and current studies, the reaction of $SiH_4 + O(^1D)$ has been carefully examined. Chemically activated SiH_3OH decomposes into various fragment species, and then some fraction of the first fragment of silanol further proceeds to the second decomposition channels. It may be reasonable to conclude that by this mechanism SiO is finally formed through a multiple-step unimolecular decomposition of the intermediates such as HSiOH, where the reaction intermediates associated with this reaction channel have a sufficiently long lifetime to distribute their internal energy statistically.

The reaction mechanism described in the current study is useful also in understanding the oxidation mechanism of silanes. Within our search, no experimental study of the reaction kinetics of SiH_3OH has been performed. Direct examination of the reaction mechanism for SiH_3OH thus will provide a very useful contribution to the improvement of the structure of integrated mechanisms,[5,6] which have been constructed on the basis of indirect information or theoretical calculations.

References and Notes

(1) Jasinski, J. M.; Gates, S. M. *Acc. Chem. Res.* **1991**, *24*, 9.

(2) Jasinski, J. M.; Meyerson, B. S.; Scott, B. A. *Annu. Rev. Phys. Chem.* **1987**, *28*, 109.

(3) Kondo, S.; Tokuhashi, K.; Nagai, H.; Iwasaka, M.; Kaise, M. *Combust. Flame* **1995**, *101*, 170.

(4) Hartman, J. R.; Famil-Ghiriha, J.; Ring, M. A.; O'Neal, H. E. *Combust. Flame* **1987**, *68*, 43.

(5) Babushok, V. I.; Tsang, W.; Burgess, D. R., Jr.; Zachariah, M. R. *Proceedings of the Twenty-Seventh Symposium (International) on Combustion*; The Combustion Institute, Pittsburgh, 1998; p 2431.

(6) Koshi, M.; Murakami, Y.; Matsui, H. *Modeling of Chemical Reaction Systems, CD-ROM Workshop Proceedings*; Heidelberg University: Germany, 1996.

(7) Koda, S.; Suga, S.; Tsuchiya, S.; Suzuki, T.; Yamada, C.; Hirota, E. *Chem. Phys. Lett.* **1989**, *161*, 35.

(8) Zachariah, E. R.; Tsang, W. *J. Phys. Chem.* **1995**, *99*, 5308.

(9) Allendorf, M. D.; Melius, C. F.; Ho, P.; Zachariah, E. R. *J. Phys. Chem.* **1995**, *99*, 15285−15293.

(10) Gordon, M. S.; Pederson, L. A. *J. Phys. Chem.* **1990**, *94*, 5527.

(11) Darling, C. L.; Schlegel, H. B. *J. Phys. Chem.* **1993**, *97*, 8207.

(12) Kudo, T.; Nagase, S. *J. Phys. Chem.* **1984**, *88*, 2833.

(13) Tachibana, A.; Sakata, K. *Appl. Surf. Sci.* **1997**, *117*, 151.

(14) Okuda, K.; Yunoki, K.; Oguchi, T.; Murakami, Y.; Tezaki, A.; Koshi, M.; Matsui, H. *J. Phys. Chem. A* **1997**, *101*, 2365.

(15) (a) Lin, J. J.; Lee, Y. T.; Yang, X. Abstract of Symposium on Chemical Kinetics and Dynamics, Okazaki, Japan, 1999; p 34. (b) Lin, J. J.; Lee, Y. T.; Yang, X. Private communication.

(16) Takahara, A.; Tezaki, A.; Matsui, H. *Bull. Chem. Soc. Jpn.*, submitted.

(17) Liszt, H. S.; Smith, W. H. *J. Quant. Spectrosc. Radiat. Transfer* **1972**, *12*, 947.

(18) Tanaka, T.; Hiramatsu, M.; Nawaka, M.; Kono, A.; Goto, T. *J. Phys. D: Appl. Phys.* **1994**, *27*, 1660.

(19) DeMore, W. B.; Sander, S. P.; Golden, D. M.; Molina, M. J.; Hampson, R. F.; Kurylo, M. J.; Howard, C. J.; Ravishankara, A. R. *Chemical kinetics and photochemical data for use in stratospheric modeling. Evaluation number 9*; JPL Publication 90-1; Jet Propulsion Laboratory, Pasadena, CA, 1990.

(20) Atkinson, R.; Baulch, D. L.; Cox, R. A.; Hampson, R. F., Jr.; Kerr, J. A.; Troe, J. *J. Phys. Chem. Ref. Data* **1992**, *21*, 1125.

(21) Swearengen, P. M.; Davis, S. J.; Niemczyk, T. M. *Chem. Phys. Lett.* **1978**, *55*, 274.

(22) Husain, D.; Norris, P. E. *J. Chem. Soc., Faraday Trans. 2* **1978**, *74*, 93.

(23) CRC Handbook of Chemistry and Physics, 76th ed.; CRC Press: Boca Raton, FL, 1995.

(24) Oddershede, J.; Elander, N. *J. Chem. Phys.* **1976**, *65*, 3495.

(25) Suzuki, G. Unpublished results in National Institute for Environmental Studies, Tsukuba, Japan. (The zero-pressure lifetime of SiO(A; $v = 0$) has been determined to be 30 ns by a direct observation of the fluorescence decay.)

(26) Wiesenfeld, J. R. *Acc. Chem. Res.* **1982**, *15*, 110.

(27) Hack, W.; Tiesemann, H. *J. Phys. Chem.* **1995**, *99*, 17364.

(28) North, S. W.; Blank, D. A.; Gezelter, J. D.; Longfellow, C. A.; Lee, Y. T. *J. Chem. Phys.* **1995**, *102*, 4447.

(29) Francisco, J. S.; Barnes, R.; Thoman, J. W., Jr. *J. Chem. Phys.* **1988**, *88*, 2334.

(30) NoorBatcha, I.; Raff, L. M.; Thompson, D. L.; Viswanathan, R. *J. Chem. Phys.* **1986**, *84*, 4341.

(31) Votintsev, V. N.; Zaslonko, I. S.; Mikheev, V. S.; Smirnov, V. N. *Kinet. Catal.* **1987**, *27*, 843.